

A Nonanuclear Copper(II) Polyoxometalate Assembled Around a μ -1,1,1,3,3,3-Azido Ligand and Its Parent Tetranuclear Complex

Pierre Mialane,^{*,[a]} Anne Dolbecq,^[a] Jérôme Marrot,^[a] Eric Rivière,^[b] and Francis Sécheresse^[a]

Dedicated to Professor D. Carillo on the occasion of his 65th birthday

Abstract: Reaction of Cu^{II} , $[\gamma\text{-SiW}_{10}\text{O}_{36}]^{8-}$, and N_3^- affords three azido polyoxotungstate complexes. Two of them have been characterized by single-crystal X-ray diffraction. Complex $\text{KNaCs}_{10}[\{\gamma\text{-SiW}_{10}\text{O}_{36}\text{Cu}_2(\text{H}_2\text{O})\text{-}(\text{N}_3)_2\}_2]\cdot 26\text{H}_2\text{O}$ (**1**) is obtained as crystals in few hours after addition of CsCl. This linear tetranuclear Cu^{II} complex consists in two $[\gamma\text{-SiW}_{10}\text{O}_{36}\text{Cu}_2\text{-}(\text{H}_2\text{O})(\text{N}_3)_2]^{6-}$ units connected through two W=O bridges. When the filtrate is left to stand for one night, a new complex is obtained. From both elemental analysis and IR spectroscopy, it has been postulated that this compound could be formulated $\text{K}_{1.5}\text{Cs}_{5.5}[\text{SiW}_{10}\text{O}_{37}\text{-}\text{Cu}_2(\text{H}_2\text{O})_2(\text{N}_3)]\cdot 14\text{H}_2\text{O}$ (**1a**), showing the loss of one azido ligand per polyoxometalate unit. Finally, when no

cesium salt is added to the reaction medium, the nonanuclear complex $\text{K}_{12}\text{Na}_7[\{\text{SiW}_8\text{O}_{31}\text{Cu}_3(\text{OH})(\text{H}_2\text{O})_2(\text{N}_3)\}_3\text{-}(\text{N}_3)]\cdot 24\text{H}_2\text{O}$ (**2**) is obtained after three days. Compound **2** crystallizes in the $R3c$ space group and consists in three $\{\text{Cu}_3\}$ units related by a C_3 axis passing through the exceptional μ -1,1,1,3,3,3-azido bridging ligand. Each trinuclear Cu^{II} unit is embedded in the $[\gamma\text{-SiW}_8\text{O}_{31}]^{10-}$ ligand, an unprecedented tetravacant polyoxometalate, showing that partial decomposition of the $[\gamma\text{-SiW}_{10}\text{O}_{36}]^{8-}$ precursor occurs with time in such experimental conditions. Mag-

netically, complex **1** behaves as two isolated $\{\text{Cu}_2(\mu_{1,1}\text{-N}_3)_2\}$ pairs in which the metal centers are strongly ferromagnetically coupled ($J = +224\text{ cm}^{-1}$, $g = 2.20$), the coupling through the W=O bridges being negligible. The magnetic behavior of complex **2** has also been studied. Relatively weak ferromagnetic couplings ($J_1 = +1.0\text{ cm}^{-1}$, $J_2 = +20.0\text{ cm}^{-1}$, $g = 2.17$) have been found inside the $\{\text{Cu}_3\}$ units, while the intertrimeric magnetic interactions occurring through the hexadentate azido ligand have been found to be antiferromagnetic ($J_3 = -5.4\text{ cm}^{-1}$) and ferromagnetic ($J_4 = +1.3\text{ cm}^{-1}$) with respect to the end-to-end and end-on azido-bridged Cu^{II} pairs, respectively.

Keywords: azides • copper • magnetic properties • polyoxometalates • tungsten

Introduction

Polyoxometalates (POMs) represent a class of metal–oxygen clusters that exhibit a unique variety of structures. Moreover, their properties make them useful in numerous fields such as medicine, catalysis, or analytical chemistry.^[1]

Due to the large number of lacunary polyanion precursors derived from the Keggin ($[\text{PW}_{12}\text{O}_{40}]^{3-}$, $[\text{SiW}_{12}\text{O}_{40}]^{4-}$) and Dawson ($[\text{P}_2\text{W}_{18}\text{O}_{62}]^{6-}$) polyanions, silicotungstates and phosphotungstates represent the most intensively studied classes of POMs. Indeed, monovacant (e.g. $[\alpha\text{-PW}_{11}\text{O}_{39}]^{7-}$, $[\alpha_1\text{-P}_2\text{W}_{17}\text{O}_{61}]^{10-}$, ...), divacant ($[\gamma\text{-SiW}_{10}\text{O}_{36}]^{8-}$) and trivacant (e.g., $[\text{A-}\alpha\text{-SiW}_9\text{O}_{34}]^{10-}$, $[\text{B-}\alpha\text{-PW}_9\text{O}_{34}]^{9-}$, ...) derivatives can be easily synthesized in one- or two-step processes in high-yield.^[2] One of the most striking abilities of these lacunary POM complexes is the encapsulation of magnetic clusters of transition-metal ions between diamagnetic fragments of metal oxides.^[3] The magnetic properties of such molecular assemblies have been extensively studied this last decade, as shown by the impressive work of Coronado's group.^[4] Complexes containing from one to four POM subunits and from one to fourteen transition-metal

[a] Dr. P. Mialane, Dr. A. Dolbecq, Dr. J. Marrot, Prof. F. Sécheresse
Institut Lavoisier
IREM, UMR 8637. Université de Versailles Saint-Quentin
45 Avenue des Etats-Unis, 78035 Versailles cedex (France)
Fax: (+33)1-39-25-43-81
E-mail: mialane@chimie.uvsq.fr

[b] Dr. E. Rivière
Laboratoire de Chimie Inorganique, UMR 8613
Institut de Chimie Moléculaire et des Matériaux d'Orsay
Université Paris-Sud, 91405 Orsay (France)

magnetic centers have been characterized. We are currently investigating the possibility of introducing exogenous ligands in the matrix of magnetic POMs. Recently, we have reported the synthesis and the characterization of $[(PW_{10}O_{37})\text{-Ni(H}_2\text{O)}_2(\text{N}_3)]^{6-}$, showing that an azido ligand can bind transition-metal cations embedded in a POM diamagnetic core.^[5] If $[(PW_{10}O_{37})(\text{Ni(H}_2\text{O)})_2(\mu\text{-N}_3)]^{6-}$ was the first azido polyoxometalate complex characterized, a very large number of organic ligand/transition metal/ N_3^- compounds, with dimensionalities ranging from discrete clusters to three-dimensional systems, have been reported so far. Indeed, the use of the N_3^- anion has been recognized as an efficient way to generate interactions between metal centers. When the azido group acts as a bridging ligand, a $\mu\text{-1,1-}$ (end-on) or a $\mu\text{-1,3-}$ coordination mode (end-to-end) is usually observed. As a general trend, the $\mu\text{-1,1-}$ mode leads to ferromagnetic coupling, and the $\mu\text{-1,3-}$ mode to antiferromagnetic coupling when the azido bridging ligand is in the basal plane.^[6] Nevertheless, a $\mu\text{-1,1-}$ antiferromagnetic complex has been recently reported,^[7] and metal cations asymmetrically bridged by $\mu\text{-1,3-}$ azido ligands can be noncoupled.^[8] In the $[(PW_{10}O_{37})(\text{Ni(H}_2\text{O)})_2(\text{N}_3)]^{6-}$ dinuclear Ni^{II} complex, the pseudohalide ligand bridges the two magnetic centers in an end-on fashion, and an $S=2$ ground state was observed. We report herein the synthesis and the structural characterization of two Cu^{II} -azido POMs, $\text{KNaCs}_{10}[\{\gamma\text{-SiW}_{10}\text{O}_{36}\text{Cu}_2(\text{H}_2\text{O})(\text{N}_3)_2\}_2]\cdot 26\text{H}_2\text{O}$ (**1**) and $\text{K}_{12}\text{Na}_7[\{\text{SiW}_8\text{O}_{31}\text{Cu}_3(\text{OH})(\text{H}_2\text{O})_2(\text{N}_3)_3(\text{N}_3)\}_3]\cdot 24\text{H}_2\text{O}$ (**2**). Complex **1** is a dimeric POM containing two $[\text{Cu}_2(\mu\text{-1,1-N}_3)]$ pairs, while **2** is formed from three $[\text{SiW}_8\text{O}_{31}]^{10-}$ subunits, an unprecedented tetravacant POM, enclosing three Cu_3 units assembled through a $\mu\text{-1,1,1,3,3,3-}$ azido ligand, a very rare bridging hexadentate coordination mode for an N_3^- ligand. The synthetic processes and the magnetic properties of these two compounds are also discussed.

Results and Discussion

Structure of $\text{KNaCs}_{10}[\{\gamma\text{-SiW}_{10}\text{O}_{36}\text{Cu}_2(\text{H}_2\text{O})(\text{N}_3)_2\}_2]\cdot 26\text{H}_2\text{O}$ (1**):** A crystal structure analysis of complex **1** has been performed on a single crystal glued in Paratone-N oil at 100 K. Complex **1** crystallizes in the monoclinic space group $P2_1/c$ (Table 1). Its structure can be described as a dimer of $[\gamma\text{-SiW}_{10}\text{O}_{36}\text{Cu}_2(\text{H}_2\text{O})(\text{N}_3)_2]^{6-}$ subunits related by an inversion center (Figure 1a). Each subunit is formed by a $[\gamma\text{-}$

Table 1. X-ray crystallographic data for **1** and **2**.

	1	2
formula	$\text{W}_{20}\text{Cu}_4\text{Cs}_{10}\text{N}_{12}\text{KNaSi}_2\text{O}_{100}\text{H}_{56}$	$\text{W}_{24}\text{Cu}_6\text{N}_{12}\text{K}_{12}\text{Na}_7\text{Si}_3\text{O}_{126}\text{H}_{63}$
M_r [g]	7202.79	7945.97
crystal system	monoclinic	rhombohedral
space group	$P2_1/c$	$R\bar{3}c$
Z	2	6
T [K]	100	293
a [Å]	11.9946(11)	18.3740(1)
b [Å]	19.0711(16)	18.3740(1)
c [Å]	23.455(2)	63.6678(1)
β [°]	99.761(5)	90
V [Å ³]	5287.7(8)	18614.77(15)
ρ_{calc} [g cm ⁻³]	4.558	4.181
μ [mm ⁻¹]	26.333	24.251
reflections collected	267587	27455
unique reflections (R_{int})	22799(0.0678)	5871(0.0841)
refined parameters	794	576
$R_1^{[a]}/wR_2^{[b]}$ [$I > 2\sigma(I)$]	0.0376/0.0903	0.0481/0.0977
$R_1^{[a]}/wR_2^{[b]}$ (all data)	0.0579/0.1024	0.0686/0.1066
largest diff. peak/hole [$e \text{ \AA}^{-3}$]	2.928/-3.384	1.983/-1.345

[a] $R_1 = \sum |F_o| - |F_c| / \sum |F_c|$; [b] $wR_2 = [\sum w(F_o^2 - F_c^2)^2 / \sum w(F_c^2)]^{1/2}$ with $1/w = \sigma^2 F_o^2 + aP^2 + bP$ and $P = F_o^2 + 2F_c^2/3$; $a = 0.0548$, $b = 0$ for **1**, $a = 0.0686$, $b = 214.57$ for **2**.

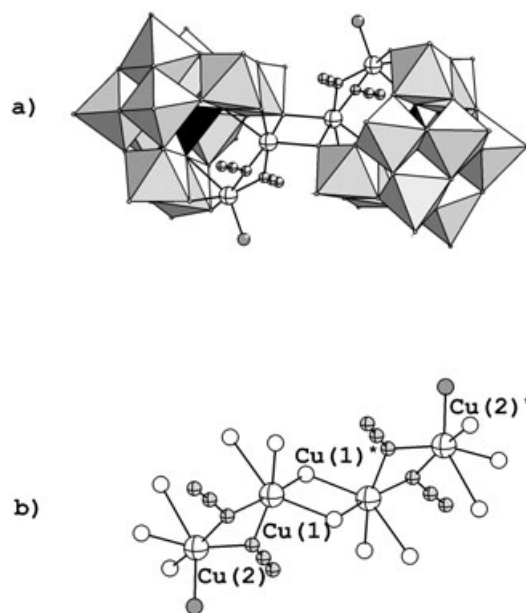


Figure 1. a) Polyhedral and ball-and-stick representation of complex **1**. b) Ball-and-stick representation of the tetranuclear Cu^{II} fragment in **1**. Light gray octahedra, WO_6 ; black octahedra, SiO_4 ; white crosshatched spheres, Cu; medium gray spheres, OH_2 ; white spheres, oxo ligand; gray crosshatched spheres, N.

$\text{SiW}_{10}\text{O}_{36}]^{8-}$ divacant polyanion coordinated to two Cu^{II} centers. These ions are bridged by two end-on azido groups. The equatorial plane of the two copper centers is defined by two terminal oxygen atoms of its $[\gamma\text{-SiW}_{10}\text{O}_{36}]^{8-}$ subunit ($d_{\text{Cu-O}} = 1.946(6)\text{--}1.982(6)$ Å) and two nitrogen atoms of the azido ligands ($d_{\text{Cu-N}} = 1.990(7)\text{--}1.999(7)$ Å). An apical position of the Cu(1) octahedron is occupied by a water molecule ($d_{\text{Cu-OH}_2} = 2.188(7)$ Å), while the corresponding position of the Cu(2) center is occupied by a terminal oxygen atom

of the adjacent $[\gamma\text{-SiW}_{10}\text{O}_{36}\text{Cu}_2(\text{H}_2\text{O})(\text{N}_3)_2]^{6-}$ unit ($d_{\text{Cu-O}} = 2.273(5)$ Å), allowing the formation of a linear tetranuclear Cu^{II} complex (Figure 1b). The sixth position of both copper centers is occupied by an oxygen atom of an $\{\text{SiO}_4\}$ group, with very long Cu–O(Si) distances ($d_{\text{Cu-O}} = 2.658(6)$ and $2.700(5)$ Å). Hence, the paramagnetic ions can be considered either in a slightly distorted square-pyramidal or in a highly axially distorted octahedral environment. The Cu(1)⋯Cu(2) separation is $2.979(1)$ Å, while the Cu(1)⋯Cu(1*) distance is equal to $3.238(4)$ Å. The Cu–N–Cu bridging angles θ are equal to $96.56(26)$ and $96.86(33)^\circ$ ($\theta_{\text{av}} = 96.71^\circ$). The topology of the $\{\text{Cu}_2(\mu_{1,1}\text{-N}_3)_2\}$ core in compound **1** is consistent with structural results obtained for other organic ligand/ $\{\text{Cu}_2(\mu_{1,1}\text{-N}_3)_2\}$ systems, with a θ_{av} value in the range of the previously reported values for only azido-bridged Cu^{II} complexes ($89.1^\circ < \theta < 104.6^\circ$).^[9] Considering POM chemistry, the $[\gamma\text{-SiW}_{10}\text{O}_{36}\text{Cu}_2(\text{H}_2\text{O})(\text{N}_3)_2]^{6-}$ subunit in **1** can be compared to the $[\gamma\text{-SiW}_{10}\text{O}_{34}\text{Mn}_2(\text{OH})_6]^{4-}$ and $[\gamma\text{-SiW}_{10}\text{O}_{36}\text{Cr}_2(\text{H}_2\text{O})_2(\text{OH})(\text{CH}_3\text{COO})_2]^{5-}$ dinuclear complexes previously reported by Pope et al.^[10] In the first compound, the two Mn^{III} centers form a $\{\text{Mn}_2(\mu\text{-OH})_2\}$ pair, analogous to the $\{\text{Cu}_2(\mu_{1,1}\text{-N}_3)_2\}$ group found in **1**, with two azido groups replacing the two hydroxo ligands. In the chromium complex, the coordination sphere of the Cr^{III} centers is different; the paramagnetic centers share a corner and the $[\gamma\text{-SiW}_{10}\text{O}_{36}]^{8-}$ part acts as a tetradentate ligand due to the presence of an additional $\mu\text{-OH}$ ligand bridging the Cr^{III} ions. Finally, it has to be noted that in **1** the shortest intermolecular Cu⋯Cu distance is $9.453(3)$ Å, longer than the Cu(2)⋯Cu(2*) intramolecular distance ($8.862(2)$ Å).

Structure of $\text{K}_{12}\text{Na}_4[\{\text{SiW}_8\text{O}_{31}\text{Cu}_3(\text{OH})(\text{H}_2\text{O})_2(\text{N}_3)_3\}_3(\text{N}_3)] \cdot 24\text{H}_2\text{O}$ (2**):** Complex **2** crystallizes in the trigonal space group $R3c$ (Table 1). Its structure consists of three equivalent $[\gamma\text{-SiW}_8\text{O}_{31}\text{Cu}_3(\text{OH})(\text{H}_2\text{O})_2(\text{N}_3)]^{6-}$ subunits related by a C_3 axis that contains the three nitrogen atoms of an encapsulated hexadentate $\mu\text{-}1,1,1,3,3,3\text{-azido}$ group (Figure 2a). The N–N–N angle is 180.0° . To our knowledge, such a bridging coordination mode for an N_3^- ligand has been previously observed only in the diamagnetic $\text{AgN}_3 \cdot 2 \text{AgNO}_3$ two-dimensional compound.^[11] Each subunit can be described as a $[\gamma\text{-SiW}_8\text{O}_{31}]^{8-}$ polyanion in which a $\{\text{W}_2\text{O}_6\}$ group has been replaced by a $\{\text{Cu}_2\text{O}(\mu_3\text{-OH})(\text{H}_2\text{O})_2(\mu_{1,3}\text{-N}_3)\}$ fragment (Figure 2b). A $\{\text{Cu}(\text{N}_3)\}$ group, with a terminal azido ligand linked to the Cu^{II} center, connects two adjacent $[\gamma\text{-SiW}_8\text{O}_{31}\text{Cu}_2(\text{OH})(\text{H}_2\text{O})_2]^{7-}$ entities by means of a $\mu_3\text{-OH}$ ligand and four Cu–O=W bonds. The resulting trinuclear $\{\text{Cu}_3\text{O}_7(\mu_3\text{-OH})(\text{H}_2\text{O})_2(\mu_{1,3}\text{-N}_3)(\text{N}_3)\}$ cluster forms a distorted defective cubane unit (Figure 2c). The Cu(1) equatorial plane is defined by two oxo ligands, a nitrogen atom of the terminal N_3^- ion, and the $\mu_3\text{-OH}$ group ($d_{\text{Cu-X}} = 2.00(3)\text{--}2.08(2)$ Å). Two oxo groups occupy the two remaining sites ($d_{\text{Cu-O}} = 2.16(2)$ and $2.19(2)$ Å). For both Cu(2) and Cu(3) ions, a $\{\text{CuO}_2(\mu_3\text{-OH})(\text{H}_2\text{O})\}$ fragment defines the equatorial plane ($d_{\text{Cu-X}} = 1.91(2)\text{--}2.01(2)$ Å), a nitrogen atom of the bridging azido ligand and an oxo group completing the coordination

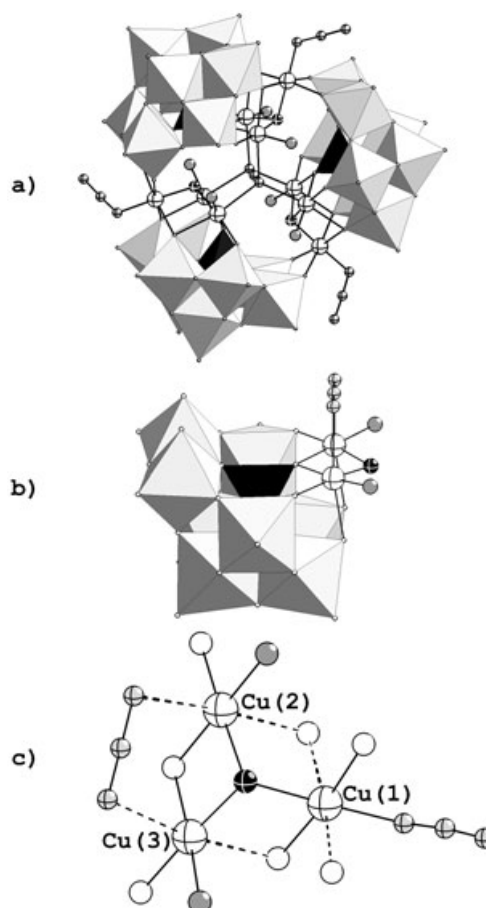


Figure 2. a) Polyhedral and ball-and-stick representation of complex **2**. b) Polyhedral and ball-and-stick representation of the $[\gamma\text{-SiW}_8\text{O}_{31}\text{Cu}_3(\text{OH})(\text{H}_2\text{O})_2(\text{N}_3)]^{6-}$ subunit in **2**. c) Ball-and-stick representation of the trinuclear Cu^{II} fragment in **2**. The dash lines indicate bonds between the metal centers and their apical ligands. Light gray octahedra, WO_6 ; black octahedra, SiO_4 ; white crosshatched spheres, Cu; medium gray spheres, OH_2 ; white spheres, oxo ligand; gray crosshatched spheres, N; black crosshatched spheres, OH.

sphere of the metal centers ($d_{\text{Cu-X}} = 2.39(2)\text{--}2.589(7)$ Å). The hexadentate N_3^- group connects the $\{\text{Cu}_3\}$ units through the three Cu(2) and the three Cu(3) ions, affording the nonanuclear Cu^{II} complex **2**. The longest intramolecular Cu⋯Cu distance is $8.655(6)$ Å and the shortest intermolecular Cu⋯Cu distance is $10.273(6)$ Å.

Synthesis and IR spectroscopy of complexes **1**, **1a**, and **2**:

The synthesis of complex **1** was achieved in relatively good yield by the reaction of Cu^{II} , $[\gamma\text{-SiW}_{10}\text{O}_{36}]^{8-}$, and a slight excess of N_3^- in dilute aqueous medium after addition of cesium chloride. Deep brown crystals of **1** suitable for single X-ray diffraction were collected after a few hours. When the filtrate was left to stand for one night at room temperature, a yellow powder was obtained (complex **1a**). Due to its insolubility, it was not possible to recrystallize this compound. Nevertheless, elemental analysis indicates that the 2:10 Cu/W ratio is maintained, but that only one azido ligand is retained in the polyoxometalate matrix. Complex **2** is obtained

in poor yield when an aqueous solution containing Cu^{II} , $[\gamma\text{-SiW}_{10}\text{O}_{36}]^{8-}$, and N_3^- was left to slowly evaporate for three days without addition of cesium chloride. Attempts to improve the yield, by variation of the temperature, the time of crystallization, and the $\text{Cu}^{\text{II}}/[\gamma\text{-SiW}_{10}\text{O}_{36}]^{8-}/\text{N}_3^-$ ratios, failed.

Vibrational spectroscopy is a very powerful tool for the determination of the coordination mode of azido ligands. In IR spectroscopy, the $\nu_{\text{as}}(\text{N}_3)$ vibration mode is observed as an intense absorption band in the 2000–2150 cm^{-1} range. The value of the stretching frequency can give a first indication on the topology of the studied complex. Indeed, general trends have been observed for divalent transition-metal complexes, allowing us to tentatively distinguish whether the N_3^- ion acts as a terminal ($\nu_{\text{as}} \sim 2040 \text{ cm}^{-1}$), end-on ($\nu_{\text{as}} \sim 2070 \text{ cm}^{-1}$), or end-to-end ($\nu_{\text{as}} \sim 2100 \text{ cm}^{-1}$) ligand.^[12] More informative is that, in addition to the anti-symmetric stretch, end-on and terminal azide complexes are expected to display a $\nu_{\text{sym}}(\text{N}_3)$ mode at $\sim 1250\text{--}1300 \text{ cm}^{-1}$. For complex **1**, two bands are observed at 2075 and 1286 cm^{-1} . This is then in agreement with the end-on coordination mode of the azido ligand found in **1** by single-crystal X-ray analysis. Considering complex **1a**, the IR spectrum shows two bands at 2078 and 1287 cm^{-1} . This indicates that an end-on coordination mode is adopted by the N_3^- ion. It is then possible to propose that **1a** can be written as $[\text{SiW}_{10}\text{O}_{37}\text{Cu}_2(\text{H}_2\text{O})_2(\mu_{1,1}\text{-N}_3)]^{7-}$ in analogy to the $[(\text{PW}_{10}\text{O}_{37})\text{Ni}_2(\text{H}_2\text{O})_2(\text{N}_3)]^{6-}$ complex,^[5] implying that isomerization occurred during the formation of **1a**; such a process has been previously observed. Indeed, Kortz et al. have reported that the reaction of $[\gamma\text{-SiW}_{10}\text{O}_{36}]^{8-}$ with Ni^{II} ions leads to the formation of the $[\{\beta\text{-SiW}_{10}\text{Ni}_2\text{O}_{36}(\text{OH})_2(\text{H}_2\text{O})\}_2]^{12-}$ species.^[13] Nevertheless, it is not possible to form an unambiguous conclusion in the absence of structural characterization.

The IR spectrum of **2** shows two moderately intense bands at 2054 and 2032 cm^{-1} and a weak band at 1294 cm^{-1} . This is in agreement with the presence of two nonequivalent azido ligands in complex **2**. With the above considerations, it is possible to assign the $\nu_{\text{as}} = 2032$ and $\nu_{\text{sym}} = 1291 \text{ cm}^{-1}$ stretches to the terminal azido ligands and the $\nu_{\text{as}} = 2054 \text{ cm}^{-1}$ stretch to the encapsulated $\mu\text{-}1,1,1,3,3,3$ -azido ligand.

We have recently reported the synthesis of the copper(II)-azido polyoxometalate $[(\text{SiW}_9\text{O}_{37})\text{Cu}_3\text{N}_3]^{11-}$.^[14] Nevertheless, the structure of this complex could not be obtained by X-ray diffraction. When this compound was dissolved in a molar NaCl solution, large crystals of the azido-free supramolecular complex $[(\text{SiW}_9\text{O}_{34})(\text{SiW}_9\text{O}_{33}(\text{OH}))(\text{Cu}(\text{OH}))_6\text{Cu}_2\text{Cl}]$ (denoted $\{\text{Cu}_{14}\}$) were obtained within minutes. In this compound, the fourteen Cu^{II} centers are assembled around a six-coordinate halide anion. Very recently, Hill's group^[15] as well as ourselves successfully synthesized the $\{\text{Cu}_{14}\}$ complex in absence of azido ligand, showing that the N_3^- ion just accelerated the crystallization process. It appears now that the role of the hexadentate chloride anion in $\{\text{Cu}_{14}\}$ is strikingly similar to that of the hexadentate azido ligand in **2**. It seems likely that the N_3^- group plays the role of a pre-assembling agent, leading in highly concentrated

halide medium to the $\{\text{Cu}_{14}\}$ complex after substitution of the azido group by a chloride anion.

Magnetic properties of $\text{KNaCs}_{10}[\gamma\text{-SiW}_{10}\text{O}_{36}\text{Cu}_2(\text{H}_2\text{O})(\text{N}_3)_2] \cdot 26\text{H}_2\text{O}$ (1**):** The magnetic behavior of compound **1** in the 2–300 K temperature range is shown in Figure 3 in the form of a $\chi_{\text{M}}T$ versus T plot, χ_{M} being the magnetic sus-

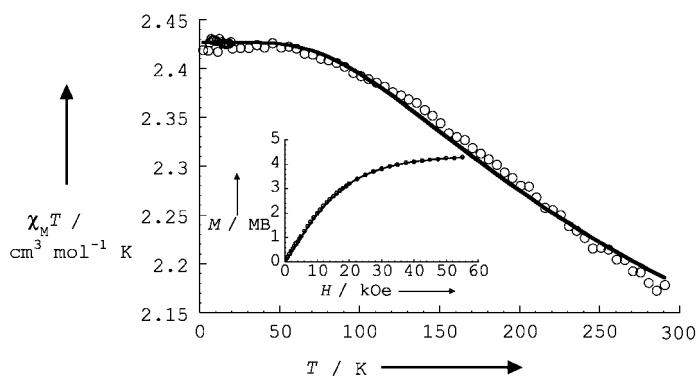
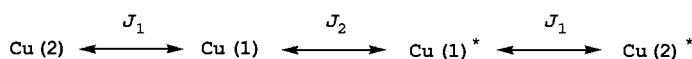


Figure 3. Plot of $\chi_{\text{M}}T$ versus T for compound **1** between 300 and 2 K. Inset: $M=f(H)$ at 2 K. The solid lines were generated from the best fit parameters given in the text.

ceptibility for one mole of **1**. At room temperature, $\chi_{\text{M}}T$ is equal to 2.18 $\text{cm}^3 \text{ mol}^{-1} \text{ K}$, a value already higher than expected for four uncoupled Cu^{II} centers ($\chi_{\text{M}}T = 1.815 \text{ cm}^3 \text{ mol}^{-1} \text{ K}$ assuming $g = 2.20$). The $\chi_{\text{M}}T=f(T)$ curve increases upon cooling, reaching a plateau around 60 K and then remains constant down to 2 K, with $\chi_{\text{M}}T = 2.42 \text{ cm}^3 \text{ mol}^{-1} \text{ K}$. This behavior is characteristic of a ferromagnetic interaction with a ground state that has a very large energy separation with respect to the first excited state. The appropriate Hamiltonian for a linear $\{\text{Cu}_4\}$ system in which half of the tetranuclear complex is symmetry related to the other half (Scheme 1)^[16] can be written as Equa-



Scheme 1.

tion (1) with $S_1 = S_2 = S_{1^*} = S_{2^*} = 1/2$, affording quintet, triplet, and singlet states.

$$\hat{H} = -J_1(\hat{S}_1\hat{S}_2 + \hat{S}_{1^*}\hat{S}_{2^*}) - J_2(\hat{S}_1\hat{S}_{1^*}) \quad (1)$$

Nevertheless, the $\chi_{\text{M}}T$ value reached at the plateau for complex **1** cannot be explained neither by considering an $S = 2$ ($\chi_{\text{M}}T = 3.63 \text{ cm}^3 \text{ mol}^{-1} \text{ K}$, assuming $g = 2.20$) nor an $S = 1$ ($\chi_{\text{M}}T = 1.21 \text{ cm}^3 \text{ mol}^{-1} \text{ K}$) ground state. Similarly, attempts to fit the $M=f(H)$ curve recorded at 2 K (Figure 3, inset) considering an $S = 1$ or $S = 2$ ground state have failed. However, an excellent fit of the magnetization curve ($g = 2.18$,

assuming $g_{\text{Cu}(1)} = g_{\text{Cu}(2)} = g$, $R = 3.2 \times 10^{-5}$)^[17] was achieved by considering two uncoupled $S=1$ pairs. Then, the magnetic behavior of compound **1** can be interpreted by considering isolated $[\gamma\text{-SiW}_{10}\text{O}_{36}\text{Cu}_2(\text{H}_2\text{O})(\text{N}_3)_2]^{6-}$ dinuclear Cu^{II} subunits (i.e., $J_2=0$). The best fitting parameters obtained from a simulation of the $\chi_{\text{M}}T=f(T)$ curve are $J_1 = +224 \text{ cm}^{-1}$ and $g = 2.20$ ($R = 1.0 \times 10^{-5}$).^[18] The J_1 value found is lower than that calculated considering the linear trend in the θ versus J plot observed by Thompson et al. ($J_1 = -41.94\theta + 4440 \text{ cm}^{-1}$),^[19] the predicted J_1 value for **1** being then $+384 \text{ cm}^{-1}$ considering $\theta = \theta_{\text{av}} = 96.71^\circ$. Nevertheless, the experimental exchange parameter is in total agreement with that found for the tetrabridged dimeric $[\text{Cu}_2(\mu_{1,1}\text{-N}_3)_2(4\text{-Ethylpyridine})_4(\mu\text{-NO}_3)_2]$ complex reported by Escuer et al.^[20] Indeed, for this compound, a J value of $+223 \text{ cm}^{-1}$ was determined for a θ angle of 97.5° , showing that the bridging nitrate ligands have no influence on the exchange parameter. Due to the lack of complexes that contain the dibridged $\{\text{Cu}(\mu\text{-O}=\text{W})_2\text{Cu}\}$ core, it is not possible to justify that J_2 is found to be negligible. Nevertheless, recently, Kortz et al. have reported^[3a] that the exchange parameter associated to such pair in the $[\text{Cu}_4\text{K}_2(\text{H}_2\text{O})_8(\alpha\text{-AsW}_9\text{O}_{33})_2]^{8-}$ complex is low ($J = +1.4 \text{ cm}^{-1}$). In **1**, the J_2 value must be even lower, as no variation of the $\chi_{\text{M}}T=f(T)$ curve is observed in the 2–10 K range. This can be tentatively justified considering that in $[\text{Cu}_4\text{K}_2(\text{H}_2\text{O})_8(\alpha\text{-AsW}_9\text{O}_{33})_2]^{8-}$, the magnetic orbitals of both copper centers forming the $\{\text{Cu}(\mu\text{-O})_2\text{Cu}\}$ fragment are involved in the magnetic exchange, while in **1**, superexchange between the Cu(1) centers occurs through the oxo ligands located in apical position.

Magnetic properties of complex $\text{K}_{12}\text{Na}_7[\{\text{SiW}_8\text{O}_{31}\text{Cu}_3(\text{OH})(\text{H}_2\text{O})_2(\text{N}_3)_3(\text{N}_3)\}\cdot 24\text{H}_2\text{O}$ (2**):** The temperature dependence of the $\chi_{\text{M}}T$ product for **2** (χ_{M} being the magnetic susceptibility per mole of **2**) in the 2–300 K temperature range is shown in Figure 4. The value of $\chi_{\text{M}}T$ at room temperature is $4.03 \text{ cm}^3 \text{ mol}^{-1} \text{ K}$; a value which is in agreement with nine magnetically isolated copper(II) ions with $g = 2.17$. Upon cooling down of the sample, $\chi_{\text{M}}T$ increases smoothly to a

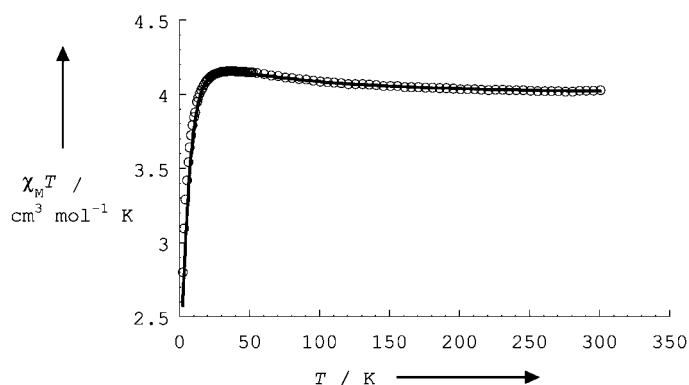
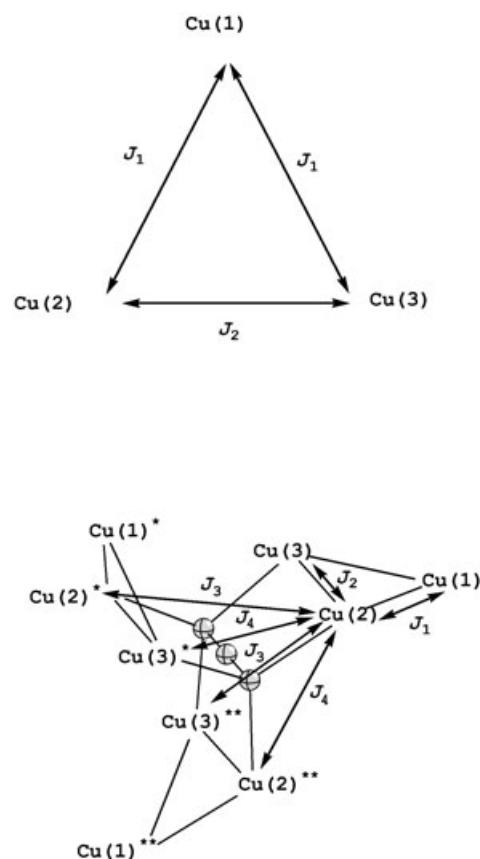


Figure 4. Plot of $\chi_{\text{M}}T$ versus T for compound **2** between 300 and 2 K. The solid line was generated from the best fit parameters given in the text considering the Hamiltonian H .

maximum value of $4.20 \text{ cm}^3 \text{ mol}^{-1} \text{ K}$ at 40 K. This behavior is indicative of a relatively weak ferromagnetic coupling. Below 40 K, $\chi_{\text{M}}T$ continuously decreases, reaching a value of $2.80 \text{ cm}^3 \text{ mol}^{-1} \text{ K}$ at 2 K. We first attempted to simulate the $\chi_{\text{M}}T=f(T)$ curve considering a simplified model, taking into account that 1) all the Cu–N distances observed between the six Cu^{II} centers and the hexadentate azido ligand are long ($d_{\text{Cu-N}} = 2.574(6)$ and $2.589(7) \text{ \AA}$), and 2) it has been shown that when the azido ligand bridges the copper(II) centers at the apical position with long Cu–ligand distances, the magnetic coupling is weak.^[21] We have then considered a model in which the three C_3 -related $[\gamma\text{-SiW}_8\text{O}_{31}\text{Cu}_3(\text{OH})(\text{H}_2\text{O})_2(\text{N}_3)]^{6-}$ subunits are magnetically noninteracting. As the Cu(2) and Cu(3) centers are in a nearly equivalent environment, the problem reduces to that of an isosceles triangle (Scheme 2, top). The appropriate Hamiltonian can be written as Equation (2) with $S_1 = S_2 = S_3 = 1/2$.

$$\hat{H} = -J_1(\hat{S}_1\hat{S}_2 + \hat{S}_1\hat{S}_3) - J_2(\hat{S}_2\hat{S}_3) \quad (2)$$



Scheme 2.

Equation (3) can then be derived from Equation (2) assuming $g_{\text{Cu}(1)} = g_{\text{Cu}(2)} = g_{\text{Cu}(3)} = g$, and in which the Weiss correction θ accounts for the interactions between the three trinuclear units and a hypothetical zero-field splitting effect on the ground state.

$$\chi_M T = \frac{3N\beta^2 g^2}{4k} \frac{T}{T-\theta} \frac{[1 + \exp(\frac{J_1-J_2}{kT}) + 10\exp(\frac{3J_1}{2kT})]}{[1 + \exp(\frac{J_1-J_2}{kT}) + 2\exp(\frac{3J_1}{2kT})]} \quad (3)$$

It has not been possible to fit the data on the whole temperature range, and the best fit, effectuated in the 7–300 K temperature range, leads to the following parameters: $g = 2.18$, $J_1 = +0.97 \text{ cm}^{-1}$, $J_2 = +16.17 \text{ cm}^{-1}$, and $\theta = -1.81 \text{ cm}^{-1}$ ($R = 1.5 \times 10^{-4}$).^[18] The determined magnitude of J_2 relative to that of J_1 seems reasonable. Indeed, the magnetic orbitals of the Cu(2) and Cu(3) metal centers, contained in the equatorial plane (Figure 2c), are directed toward the μ -OH and μ -O ligands bridging these two cations. Nevertheless, this model cannot be validated, as it is found that the mean field parameter is stronger than J_1 . This indicates that the magnetic interactions between the $[\gamma\text{-SiW}_8\text{O}_{31}\text{Cu}_3(\text{OH})(\text{H}_2\text{O})_2(\text{N}_3)]^{6-}$ units cannot be neglected. Therefore, a model considering the nine exchange-coupled paramagnetic centers has been studied. This model introduces two additional exchange parameters J_3 and J_4 related to the coupling of the Cu^{II} ions through the hexadentate azido ligand. Considering that the Cu(2) and Cu(3) metal centers are in a nearly equivalent environment, the coupling scheme involving Cu(3) can be deduced from that represented for Cu(2) in Scheme 2 (bottom). The parameter J_3 is related to end-to-end magnetic interactions, while J_4 reflects μ -1,1-coupling pathways. In both cases, an apical–apical coordination mode is adopted by the azido bridging ligand. The appropriate Hamiltonian is then defined as Equation (4).

$$\begin{aligned} \hat{H}' = & -J_1(\hat{S}_{\text{Cu}(1)}\hat{S}_{\text{Cu}(2)} + \hat{S}_{\text{Cu}(1)}\hat{S}_{\text{Cu}(3)} + \hat{S}_{\text{Cu}(1)}\hat{S}_{\text{Cu}(2)*} + \hat{S}_{\text{Cu}(1)*}\hat{S}_{\text{Cu}(3)*} \\ & + \hat{S}_{\text{Cu}(1)**}\hat{S}_{\text{Cu}(2)**} + \hat{S}_{\text{Cu}(1)**}\hat{S}_{\text{Cu}(3)**}) - J_2(\hat{S}_{\text{Cu}(2)}\hat{S}_{\text{Cu}(3)} + \hat{S}_{\text{Cu}(2)*}\hat{S}_{\text{Cu}(3)*} \\ & + \hat{S}_{\text{Cu}(2)**}\hat{S}_{\text{Cu}(3)**}) - J_3(\hat{S}_{\text{Cu}(2)}\hat{S}_{\text{Cu}(2)*} + \hat{S}_{\text{Cu}(2)}\hat{S}_{\text{Cu}(3)**} + \hat{S}_{\text{Cu}(3)}\hat{S}_{\text{Cu}(2)**} \\ & + \hat{S}_{\text{Cu}(3)}\hat{S}_{\text{Cu}(3)*} + \hat{S}_{\text{Cu}(2)*}\hat{S}_{\text{Cu}(2)**} + \hat{S}_{\text{Cu}(2)*}\hat{S}_{\text{Cu}(3)*}) - J_4(\hat{S}_{\text{Cu}(2)}\hat{S}_{\text{Cu}(2)**} \\ & + \hat{S}_{\text{Cu}(2)}\hat{S}_{\text{Cu}(3)*} + \hat{S}_{\text{Cu}(3)*}\hat{S}_{\text{Cu}(2)**} + \hat{S}_{\text{Cu}(3)}\hat{S}_{\text{Cu}(2)*} + \hat{S}_{\text{Cu}(3)*}\hat{S}_{\text{Cu}(3)**} \\ & + \hat{S}_{\text{Cu}(2)*}\hat{S}_{\text{Cu}(3)**}) \end{aligned} \quad (4)$$

The magnetic susceptibility has been computed by using the procedure developed by Borràs-Almenar and co-workers (MAGPACK program).^[22] The best-fitting parameters are $J_1 = +1.0 \text{ cm}^{-1}$, $J_2 = +20.0 \text{ cm}^{-1}$, $J_3 = -5.4 \text{ cm}^{-1}$, $J_4 = +1.3 \text{ cm}^{-1}$, and $g = 2.17$. First, it has to be mentioned that the J_1 and J_2 values determined by considering \hat{H}' are similar to those determined by considering \hat{H} , keeping in mind that the determination of J from the magnetic data is much more accurate for $J < 0$ than for $J > 0$.^[23] Secondly, as expected, the determined J_3 and J_4 values correspond to weak magnetic couplings.

Successful correlation of the superexchange coupling as a function of bond and torsion angles related to single μ -1,3-azido bridge has been performed by using extended Hückel methods, showing that the M–N distance is a less significant parameter.^[24] We must point out here that in our model, in order to avoid overparametrization, the J_3 parameter is re-

lated to all the Cu^{II} pairs coupled through the central azido ligand in an end-to-end fashion, irrespective of the torsion angle. Focusing then on the M–N–N bond angle, it has been demonstrated by Escuer et al. that, for d⁸ and d⁹ ions, weak ferromagnetism is expected for large angles ($\theta > 160^\circ$), anti-ferromagnetism being expected for lower angles. Our result ($J_3 = -5.40 \text{ cm}^{-1}$ for $\theta = 96.42(8)–97.73(8)^\circ$) is then in agreement with this prediction.

It is not realistic to compare the magnetic behavior of basal–basal and apical–apical end-on azido bridged complexes. On the other hand, while very few apical–apical μ -1,1-azido-bridged complexes have been characterized to date,^[21] several apical–basal end-on azido-bridged complexes have been reported.^[25] Nevertheless, no clear magnetostructural correlations have been found to date, and we can only underline that the J_4 value is in the range of the exchange constants determined for such compounds. All these considerations tend to validate the approach used for the simulation of the magnetic behavior of compound **2**.

Conclusion

In this work, we have shown that the reaction of Cu^{II}, $[\gamma\text{-SiW}_{10}\text{O}_{36}]^{8-}$, and N_3^- can afford three different azido polyoxometalate complexes that can be selectively isolated at different reaction steps. Even if complex **2** is a minor product, it can be isolated selectively in absence of the cesium cation, due to its higher insolubility compared to complexes **1** and **1a**. The azido ligand can either connect magnetic centers inside the POM complexes or lead to the supramolecular assembling of several POM units. From a magnetic point of view, complex **1** represents the strongest ferromagnetically coupled POM. In order to obtain high-spin polyoxometalate molecular complexes, we are currently working on the extension of this new POM family to other first-row transition metals. To date, it has not been possible to obtain such compounds in aqueous medium. Nevertheless, our first attempts to perform analogous reactions in organic media have shown promising results.

Experimental Section

$\text{K}_8[\gamma\text{-SiW}_{10}\text{O}_{36}] \cdot 12\text{H}_2\text{O}$ was prepared as previously described.^[2]

Synthesis of $\text{KNaCs}_{10}[\{\gamma\text{-SiW}_{10}\text{O}_{36}\text{Cu}_2(\text{H}_2\text{O})(\text{N}_3)_2\}_2] \cdot 26\text{H}_2\text{O}$ (1): In an 80 mL beaker, $\text{CuCl}_2 \cdot 2\text{H}_2\text{O}$ (0.057 g, 3.34×10^{-4} mol) in water (10 mL) was added to a suspension of $\text{K}_8[\gamma\text{-SiW}_{10}\text{O}_{36}] \cdot 12\text{H}_2\text{O}$ (0.500 g, 1.67×10^{-4} mol) in water (10 mL). After 1 min, NaN_3 (0.057 g, 8.77×10^{-4} mol) in water (10 mL) was added, followed immediately by the addition of CsCl (0.500 g, 2.97×10^{-3} mol) in water (10 mL). The solution was quickly transferred in a 10 cm \varnothing crystallizing dish and was left to stand at room temperature. After 2–3 h, brown needle crystals suitable for X-ray diffraction were collected. Yield: 0.255 g (42%, based on Cu); IR (KBr pellets): $\tilde{\nu} = 2075$ (s), 1614 (m), 1301 (sh), 1286 (w), 1001 (m), 986 (w), 942 (s), 912 (s), 894 (s), 857 (s), 781 (s), 724 (s), 639 (m), 588 (m), 528 (m), 483 (w), 402 (m), 381 (m), 360 (m), 343 (m), 314 cm^{-1} (m); elemental analysis calcd (%) for $\text{W}_{20}\text{Cu}_4\text{Cs}_{10}\text{N}_{12}\text{KNaSi}_2\text{O}_{100}\text{H}_{56}$: W 51.05, Cu 3.53,

Cs 18.45, N 2.33, K 0.54, Na 0.32; found: W 50.89, Cu 3.72, Cs 18.49, N 2.13, K 0.43, Na 0.12.

The filtrate was then left to stand at room temperature, and after one night a fine yellow powder (**1a**) was filtered and thoroughly washed with water, in order to remove any water soluble complex **1**, ethanol, and diethyl ether (yield : 210 mg). IR (KBr pellets): $\tilde{\nu}$ = 2078 (s), 1623 (m), 1287 (w), 1262 (w), 987 (m), 937 (s), 895 (sh), 874 (s), 791 (s), 760 (s), 742 (s), 546 (m), 523 (m), 366 cm^{-1} (m); elemental analysis calcd (%) for $\text{K}_{1.5}\text{Cs}_{5.5}[\text{SiW}_{10}\text{O}_{37}\text{Cu}_2(\text{H}_2\text{O})_2(\text{N}_3)_3]\cdot 14\text{H}_2\text{O}$: W 49.61, Cu 3.43, Cs 19.73, N 1.13, K 1.58; found: W 49.58, Cu 3.63, Cs 18.86, N 0.85, K 1.20.

K₁₂Na₇[SiW₈O₃₁Cu₃(OH)(H₂O)₂(N₃)₃]-24H₂O (2**):** $\text{Cu}(\text{NO}_3)_2\cdot 3\text{H}_2\text{O}$ (0.160 g, 6.64×10^{-4} mol) in water (5 mL) was added to a suspension of $\text{K}_3[\gamma\text{-SiW}_{10}\text{O}_{36}]\cdot 12\text{H}_2\text{O}$ (1 g, 3.33×10^{-4} mol) in water (10 mL). NaN_3 (0.076 g, 1.17×10^{-3} mol) in water (5 mL) was then added, and the solution was left to evaporate slowly at room temperature. After 3 days, green yellow crystals suitable for X-ray diffraction were easily separated by decantation from a fine yellow powder and collected. Yield: 0.060 g (10%, based on Cu); IR (KBr pellets): $\tilde{\nu}$ = 2054 (m), 2032 (m), 1625 (m), 1294 (w), 1130 (w), 998 (m), 941 (s), 872 (s), 798 (s), 732 (s), 699 (s), 548 (m), 520 (m), 402 (m), 352 cm^{-1} (m); elemental analysis calcd (%) for $\text{W}_{24}\text{Cu}_9\text{N}_{12}\text{K}_{12}\text{Na}_7\text{Si}_5\text{O}_{126}\text{H}_{63}$: W 55.53, Cu 7.20, K 5.90; found: W 55.52, Cu 7.18, K 6.01.

Magnetic measurements: Magnetic susceptibility measurements were carried out with a Quantum Design SQUID Magnetometer with an applied field of 1000 G. The independence of the susceptibility value with regard to the applied field was checked at room temperature. The susceptibility data were corrected from the diamagnetic contributions as deduced by using Pascal's constant tables.

X-ray crystallography: Intensity data collection was carried out with a Siemens SMART diffractometer for complex **1** and with a Bruker Nonius X8 APEX 2 diffractometer for complex **2**, each equipped with a CCD detector, using MoK_α monochromatized radiation ($\lambda = 0.71073 \text{ \AA}$). Due to its high instability, a single crystal of complex **1** was mounted on a fiber glass in Paratone-N oil and intensity data collection was performed at 100 K. The absorption correction was based on multiple and symmetry-equivalent reflections in the data set by using the SADABS program based on the method of Blessing. The structure was solved by direct methods and refined by full-matrix least-squares using the SHELX-TL package. For complex **1** and **2**, some disordered alkaline counterions and free water molecules have been refined isotropically, the

Table 2. Selected bond lengths [\AA] for **1** and **2**.

	1	2
Cu(1)–O _{eq}	1.946(6), 1.980(6)	2.01(2), 2.026(19), 2.08(2)
Cu(1)–O _{ax}	2.188(7), 2.700(5)	2.16(2), 2.19(2)
Cu(2)–O _{eq}	1.960(6), 1.982(6)	1.96(2), 1.966(19), 1.97(2), 2.01(2)
Cu(2)–O _{ax}	2.273(5), 2.658(6)	2.39(2)
Cu(3)–O _{eq}		1.91(2), 1.95(2), 1.98(2), 1.999(17)
Cu(3)–O _{ax}		2.41(2)
Cu(1)–N	1.993(7), 1.999(7)	2.00(3)
Cu(2)–N	1.990(7), 1.992(7)	2.574(6)
Cu(3)–N		2.589(7)
Cu(1)⋯Cu(1)	3.238(4)	
Cu(1)⋯Cu(2)	2.979(1)	3.181(6)
Cu(2)⋯Cu(3)		2.967(5)
Cu(1)⋯Cu(3)		3.157(6)
Si–O	1.625(6)–1.654(6) [1.637] ^[a]	1.594(19)–1.64(2) [1.625]
W–O _a ^[b]	2.246(6)–2.346(5) [2.297]	2.253(17)–2.399(18) [2.333]
W–O _{bc} ^[b]	1.795(6)–2.089(6) [1.922]	1.76(2)–2.14(2) [1.917]
W–O _d ^[b]	1.723(6)–1.738(6) [1.728]	1.67(2)–1.73(2) [1.703]

[a] Mean values are indicated between square brackets. [b] O_a refers to an oxygen atom of the central cavity, bound to the silicon atom; O_{bc} refers to bridging oxygen atoms; O_d refers to a terminal oxygen atom.

other atoms being refined anisotropically. Crystallographic data are given in Table 1. Selected bond lengths are listed in Table 2. Further details of the crystal structure investigations may be obtained from the Fachinformationszentrum Karlsruhe, 76344 Eggenstein-Leopoldshafen, Germany (fax: (+49)7247–808–666; e-mail: crystdata@fiz-karlsruhe.de) on quoting the depository numbers CSD-414257 (**1**) and CSD-414258 (**2**).

- [1] a) M. T. Pope, *Heteropoly and Isopoly Oxometalates*, Springer, Berlin (Germany), **1983**; b) special issue on Polyoxometalates: *Chem. Rev.* **1998**, *98* (Guest Ed.: C. Hill); c) *Polyoxometalate Chemistry: From Platonic Solids to Anti-Retroviral Activity* (Eds.: M. T. Pope, A. Müller), Kluwer, Dordrecht (The Netherlands), **1994**.
- [2] *Inorganic Syntheses, Vol. 27* (Ed.: A. P. Ginsbergh), Wiley, **1990**, p. 88.
- [3] For recent articles reporting vacant polyoxotungstates enclosing paramagnetic ions, see: a) U. Kortz, S. Nellutla, A. C. Stowe, N. S. Dalal, J. van Tol, B. S. Bassil, *Inorg. Chem.* **2004**, *43*, 144; b) J. M. Clemente-Juan, E. Coronado, A. Forment-Aliaga, J. R. Galan-Mascaros, C. Gimenez-Saiz, C. J. Gomez-Garcia, *Inorg. Chem.* **2004**, *43*, 2689; c) U. Kortz, S. Nellutla, A. C. Stowe, N. S. Dalal, U. Rauwald, W. Danquah, D. Ravot, *Inorg. Chem.* **2004**, *43*, 2308; d) N. Laronze, J. Marrot, G. Hervé, *Inorg. Chem.* **2003**, *42*, 5857; e) I. M. Mbomekalle, B. Keita, M. Nierlich, U. Kortz, P. Berthet, L. Nadjo, *Inorg. Chem.* **2003**, *42*, 5143; f) N. M. Okun, T. M. Anderson, C. L. Hill, *J. Am. Chem. Soc.* **2003**, *125*, 3194; g) I. M. Mbomekalle, B. Keita, L. Nadjo, P. Berthet, K. I. Hardcastle, C. L. Hill, T. M. Anderson, *Inorg. Chem.* **2003**, *42*, 1163.
- [4] J. M. Clemente-Juan, E. Coronado, *Coord. Chem. Rev.* **1999**, *193–195*, 361.
- [5] P. Mialane, A. Dolbecq, E. Rivière, J. Marrot, F. Sécheresse, *Angew. Chem.* **2004**, *116*, 2324; *Angew. Chem. Int. Ed.* **2004**, *43*, 2274.
- [6] For a review on Ni^{II} and Mn^{II} azido bridge complexes, see J. Ribas, A. Escuer, M. Monfort, R. Vicente, R. Cortés, L. Lezama, T. Rojo, *Coord. Chem. Rev.* **1999**, *193–195*, 1027.
- [7] S. Koner, S. Saha, T. Mallah, K.-I. Okamoto, *Inorg. Chem.* **2004**, *43*, 840.
- [8] I. Bkouche-Waksman, S. Sikorav, O. Kahn, *J. Crystallogr. Spectrosc. Res.* **1983**, *13*, 303.
- [9] a) O. Kahn, S. Sikorav, J. Gouteron, S. Jeannin, Y. Jeannin, *Inorg. Chem.* **1984**, *23*, 490; b) J. Comarmond, P. Plumeré, J.-M. Lehn, Y. Agnus, R. Louis, R. Weiss, O. Kahn, I. Morgenstern-Badarau, *J. Am. Chem. Soc.* **1982**, *104*, 6330; c) S. S. Tandon, L. K. Thompson, E. M. Manuel, J. N. Bridson, *Inorg. Chem.* **1994**, *33*, 5555; d) G. A. Van Albada, M. T. Lakin, N. Veldman, A. L. Spek, J. Reedijk, *Inorg. Chem.* **1995**, *34*, 4910.
- [10] a) K. Wassermann, H.-J. Lunk, R. Palm, J. Fuchs, N. Steinfeldt, R. Stösser, M. T. Pope, *Inorg. Chem.* **1996**, *35*, 3273; b) X.-Y. Zhang, C. J. O'Connor, G. B. Jameson, M. T. Pope, *Inorg. Chem.* **1996**, *35*, 30.
- [11] G.-C. Guo, T. C. W. Mak, *Angew. Chem.* **1998**, *110*, 3460; *Angew. Chem. Int. Ed. Engl.* **1998**, *37*, 3268.
- [12] R. Cortés, M. Drillon, X. Solans, L. Lezama, T. Rojo, *Inorg. Chem.* **1997**, *36*, 677.
- [13] U. Kortz, Y. Jeannin, A. Tézé, G. Hervé, S. Isber, *Inorg. Chem.* **1999**, *38*, 3670.
- [14] P. Mialane, A. Dolbecq, J. Marrot, E. Rivière, F. Sécheresse, *Angew. Chem.* **2003**, *115*, 3647; *Angew. Chem. Int. Ed.* **2003**, *42*, 3523.
- [15] Dr. T. M. Anderson, personal communication.
- [16] The stars refer to crystallographically equivalent paramagnetic centers.
- [17] $R = [\sum(M_{\text{calcd}} - M_{\text{obsd}})^2 / \sum(M_{\text{obsd}})^2]$.
- [18] $R = [\sum(\chi_M T_{\text{calcd}} - \chi_M T_{\text{obsd}})^2 / \sum(\chi_M T_{\text{obsd}})^2]$.
- [19] L. K. Thompson, S. S. Tandon, M. E. Manuel, *Inorg. Chem.* **1995**, *34*, 2356.
- [20] A. Escuer, M. A. S. Goher, F. A. Mautner, R. Vicente, *Inorg. Chem.* **2000**, *39*, 2107.
- [21] M. Mikuriya, S. Kida, I. Murase, *Bull. Chem. Soc. Jpn.* **1987**, *60*, 1355.

- [22] a) J. J. Borràs-Almenar, J. M. Clemente-Juan, E. Coronado, B. S. Tsukerblat, *Inorg. Chem.* **1999**, *38*, 6081; b) J. J. Borràs-Almenar, J. M. Clemente-Juan, E. Coronado, B. S. Tsukerblat, *J. Comput. Chem.* **2001**, *22*, 985.
- [23] O. Kahn, *Molecular Magnetism*, VCH, New York, **1993**.
- [24] a) A. Escuer, R. Vicente, J. Ribas, M. S. El Fallah, X. Solans, M. Font-Bardía, *Inorg. Chem.* **1993**, *32*, 3727; b) A. Escuer, R. Vicente, J. Ribas, M. S. El Fallah, X. Solans, M. Font-Bardía, *J. Chem. Soc. Dalton Trans.* **1996**, 1013; c) A. Escuer, C. J. Harding, Y. Dussart, J. Nelson, V. McKee, R. Vicente, *J. Chem. Soc. Dalton Trans.* **1999**, 223.
- [25] see M. S. Ray, A. Ghosh, R. Bhattacharya, G. Mukhopadhyay, M. G. B. Drew, J. Ribas, *Dalton Trans.* **2004**, 252, and references therein.

Received: July 27, 2004
Published online: January 25, 2005